Electron and hole g factors in InAs/InAlGaAs self-assembled quantum dots emitting at telecom wavelengths

V.V. Belykh,[1,*] A. Greilich,[1] D.R. Yakovlev,[1,2] M. Yacob,[3] J.P. Reithmaier,[3] M. Benyoucef,[3] and M. Bayer[1,2]

[1] *Experimentelle Physik 2, Technische Universität Dortmund, D-44221 Dortmund, Germany*
[2] *Ioffe Institute, Russian Academy of Sciences, 194021 St. Petersburg, Russia*
[3] *Institute of Nanostructure Technologies and Analytics (INA), CINSaT, University of Kassel, Heinrich-Plett-Str. 40, D-34132 Kassel, Germany*

(Dated: October 9, 2015)

We extend the range of quantum dot (QD) emission energies where electron and hole g factors have been measured to the practically important telecom range. The spin dynamics in InAs/$In_{0.53}Al_{0.24}Ga_{0.23}As$ self-assembled QDs with emission wavelengths at about 1.6 μm grown on InP substrate is investigated by pump-probe Faraday rotation spectroscopy in a magnetic field. Pronounced oscillations on two different frequencies, corresponding to the QD electron and hole spin precessions about the field are observed from which the corresponding g factors are determined. The electron g factor of about -1.9 has the largest negative value so far measured for III-V QDs by optical methods. This value, as well as the g factors reported for other III-V QDs, differ from those expected for bulk semiconductors at the same emission energies, and this difference increases significantly for decreasing energies.

PACS numbers: 78.47.D-, 78.67.Hc, 78.55.Cr

doi:10.1103/PhysRevB.92.165307

arXiv:1510.02408v1 [cond-mat.mes-hall] 8 Oct 2015

I. INTRODUCTION

Spin physics has attracted great attention in recent years, inspired by the possibility of using electron or hole spins for storing and encoding quantum information [1]. Semiconductor quantum dots (QDs) provide an appropriate platform for manipulating a carrier spin, in particular, that of an electron. The spatial confinement of electrons in QDs suppresses the most efficient spin relaxation mechanisms [2] and results in long spin coherence times [3]. One of the most important parameters for the spin control is the g factor, which characterizes the susceptibility of a spin to a magnetic field. In semiconductors, electrons are quasiparticles and their g factor might be drastically different from the $g_0 \approx 2$ of a free electron. g factors in QDs have been measured either electrically [4–11] or optically [12–26]. The most widespread optical method is the measurement of the Zeeman splitting in magnetoluminescence spectra which, in general, gives only the exciton g factor [12–18]. However, in some cases, reduced symmetry of the QDs has allowed one to observe also the dark exciton states and separate electron and hole g factor contributions [12, 13]. Other optical methods of g factor determination are spin noise spectroscopy [25] and spin-flip Raman scattering [26]. Especially high precision in the measurement can be achieved with optical pump-probe spectroscopy, where the g factor is determined from the frequency of spin polarization oscillations in a perpendicular magnetic field [19–24]. Pump-probe spectroscopy allows one to determine separately the electron and hole g factors as well as the g factor spread, which contributes to the decay of the oscillations [20]. Furthermore, the spin mode-locking effect in the pump-probe signal enables one to evaluate the spin coherence time T_2 and study the dynamics of the nuclear spin polarization [3, 27].

So far, electron and hole g factors have been measured for QDs emitting in the energy range $E \gtrsim 1.0$ eV. Moreover, in pump-probe experiments, g factors have been measured only for $E \gtrsim 1.3$ eV, the energies accessible by a Ti:sapphire laser. However, an important energy range from a practical point of view is the telecommunication range which covers $0.75\ \text{eV} \lesssim E \lesssim 0.95$ eV ($1.3-1.7\ \mu$m), corresponding to the transparency window of an optical fiber. Furthermore, the spin dynamics in QDs with low band-gap energies is of fundamental interest as it can be used to test the existing theories of g factors in QDs [28–31] and stimulate the development of novel approaches, which in turn can help in refining band structure parameters. In particular, large in magnitude, negative electron g factors are expected for small band-gap energies so that they may help to study and implement new robust spin interaction effects in QDs [32, 33].

In this paper we measure the electron and hole g factors, g_e and g_h, for QDs emitting around 0.8 eV (1.6 μm) by using the pump-probe Faraday ellipticity (analogous to the Faraday rotation) technique. The obtained electron and hole g factors have the largest absolute values measured so far for III-V QDs by optical methods. We also systemize the values of electron g factors $g_e^{QD}(E)$ for III-V QDs with widely varying emission energies E and show that $g_e^{QD}(E) > g_e^{bulk}(E)$, where $g_e^{bulk}(E)$ is the electron g factor in bulk materials calculated according to the Roth-Lax-Zwerdling relation [34] (which gives good agreement for the electron g factors measured in bulk semiconductors [35]). The electron g factor in QDs depends not only on the transition energy E, as it is the case for the longitudinal electron g factor in QWs [36],

* vasilii.belykh@tu-dortmund.de

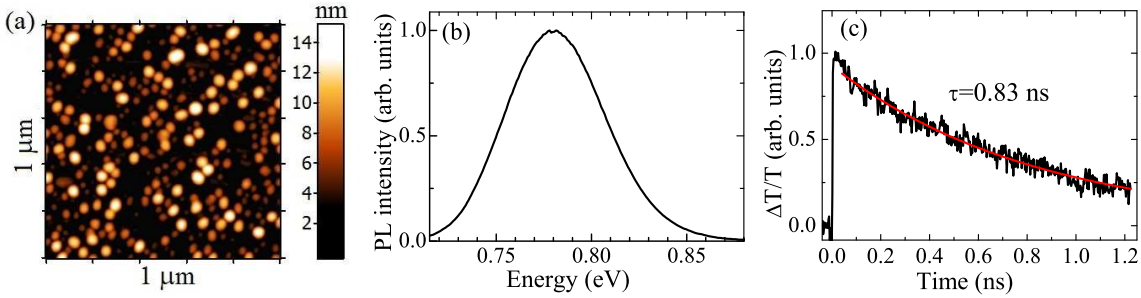

FIG. 1. (a) Atomic force microscopy image of an InAs QD layer deposited on an $In_{0.53}Al_{0.24}Ga_{0.23}As$ barrier. (b) Photoluminescence spectrum of the studied InAs/$In_{0.53}Al_{0.24}Ga_{0.23}As$ QDs at $T = 10$ K. (c) Dynamics of the QDs relative transmission measured with a laser energy of 0.79 eV and spectral width of 10 meV at $T = 12$ K. The red line shows the exponential fit to the experimental data.

but is also determined by the QD shape and composition, and can provide information on these parameters.

II. EXPERIMENTAL DETAILS

The sample under study was grown by molecular-beam epitaxy on a (100)-oriented InP substrate and contains 5.5 monolayers of InAs surrounded by $In_{0.53}Al_{0.24}Ga_{0.23}As$ barriers. The bottom barrier contains a Si δ-doped layer at a distance of 15 nm from the InAs layer. The InAs layer is transformed into self-assembled QDs with a density of about 10^{10} cm^{-2}. An atomic force microscopy image of the InAs QD layer on top of the $In_{0.53}Al_{0.24}Ga_{0.23}As$ barrier is shown in Fig. 1(a). From previous studies of similar structures it is known that the medium and large sized QDs are optically active, while the background dots of small size are optically inactive [37]. The average diameter and height of the optically active QDs are about 50 and 13 nm, respectively. A photoluminescence (PL) spectrum of such a QD ensemble taken at temperature $T = 10$ K is shown in Fig. 1(b). The emission is centered at $\sim$ 0.8 eV (~ 1.6 μm) with an inhomogeneous broadening originating from the spread of QD parameters.

The sample is placed in a split-coil magneto-cryostat at $T = 7$ K. Magnetic fields up to $B = 4$ T are applied in the Voigt geometry (parallel to the sample surface, perpendicular to the light wave vectors) unless otherwise stated. A pump-probe technique with polarization sensitivity is employed to measure the spin dynamics. We use a NT&C laser system consisting of an optical parametric amplifier (OPA) pumped by a mode-locked Yb:KGW laser operating at 1040 nm [38]. The laser system generates a periodic train (emission pulse frequency 40 MHz) of 300-fs-long pulses at a tunable wavelength of $1350 - 4500$ nm. By means of a pulse shaper, the broad (~ 60 nm) spectrum is shaped down to a width of 10 nm (5 meV) centered at the desired wavelength (1570 nm), unless otherwise stated. The laser output is split into pump and probe beams. The circular-polarized pump generates the carrier spin polarization whose temporal evolution is probed by measuring the ellipticity of the probe beam, which is initially linearly polarized, after transmission through the sample. This method is analogous to measuring the Faraday rotation of the probe beam and provides similar information [39]. In all experiments, except those where the pump power dependence of the signal strength is measured, nearly π-pulse excitation power leading to maximal spin polarization is used.

The population dynamics of the optically injected electron-hole pairs in the QDs is investigated by measuring the differential transmission $\Delta T/T$ in a pump-probe experiment (Fig. 1(c)). Linearly polarized pump pulses are used to excite a carrier population that was monitored by the polarized probe pulses as a function of delay relative to the pumps. Pump and probe pulses have orthogonal linear polarizations to avoid polarization interference and have the same photon energy centered around the maximum of the PL spectrum of the QDs. The obtained dynamics of the transmission (see Fig. 1(c)) shows, to a good approximation, a monoexponential decay corresponding to an exciton recombination time of 0.83 ns.

III. RESULTS AND DISCUSSION

Figure 2(a) shows the dynamics of the ellipticity signal recorded on the InAs quantum dot sample for different magnetic fields. The traces show oscillations on two frequencies as evidenced by the fast Fourier transform (FFT) spectrum of the ellipticity dynamics at $B = 1$ T shown in the inset of Fig. 2(a). As we will show below, the fast and slow oscillations can be attributed to the electron and hole spin precessions, respectively. The dynamics are fitted by a form representing the sum of two oscillating functions of type $\cos(\omega t)\exp(-t^2/2T_2^{*2})$, where t is the delay time, ω is the oscillation frequency, and T_2^* is the spin dephasing time. The fits are shown by the red dotted lines in Fig. 2(a). The Gaussian type of the oscillation decay $\exp(-t^2/2T_2^{*2})$ reflects the Gaus-

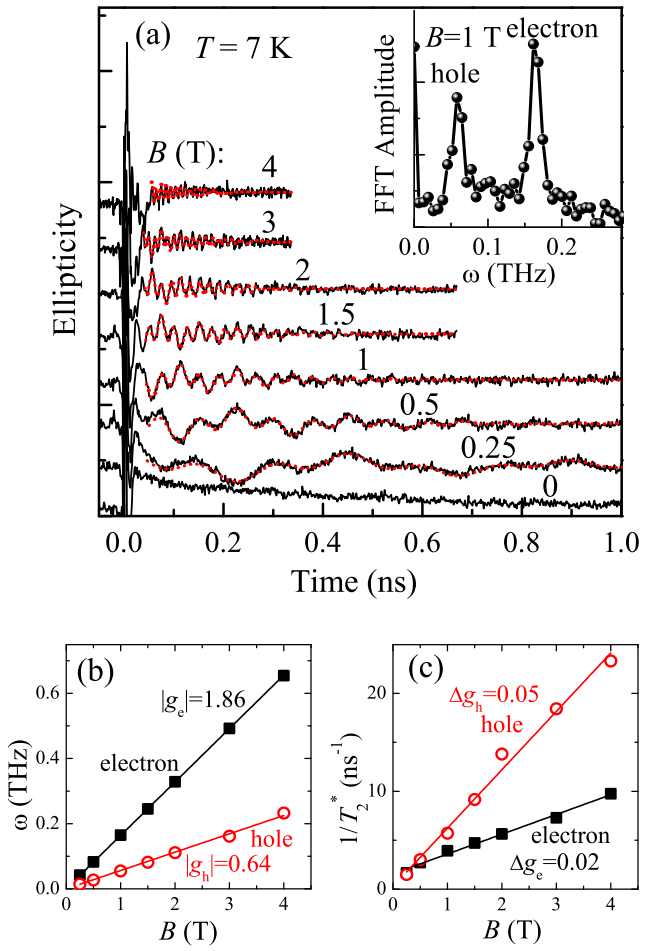

FIG. 2. (a) Dynamics of the ellipticity signal at different magnetic fields. The red dotted lines show fits to the experimental data. The form of the fit is given by the sum of two damped oscillating functions. The curves are shifted vertically for clarity. The inset shows a FFT spectrum of the ellipticity signal at $B = 1$ T. (b),(c) Magnetic field dependencies of the oscillation frequencies (b) and decay rates (c) for the fast (solid squares) and slow (open circles) oscillations in the spin dynamics. The laser photon energy is set to 0.79 eV.

sian spread of a g factor $\exp[-(g-g_0)^2/2\Delta g^2]$ [40]. This spread is assumed to be the main source of the observed damping of the ellipticity signal in the magnetic field. While the g factor determines the oscillation frequency $\omega = |g|\mu_B B/\hbar$, the spread of the g factor determines the damping rate $T_2^{*-1} = \Delta g \mu_B B/\hbar$, where μ_B is the Bohr magneton. The other possible source of the oscillation damping is fluctuations in the nuclear spin bath in the quantum dot [41]. Their contribution, however, shows up only for magnetic fields much weaker than the B considered here. Note that oscillations are observed only within the carrier lifetime (≈ 0.83 ns) which also limits the spin coherent signal in QDs without resident carriers (uncharged QDs).

The dependencies of the oscillation frequencies on the magnetic field are shown in Fig. 2(b). They give the following values of the transverse g factors: $|g_e| = 1.86$ for the fast (electron) oscillations and $|g_h| = 0.64$ for the slow (hole) oscillations. Figure 2(c) shows the dependencies of the damping rates T_2^{*-1} on the magnetic field. They are close to linear, confirming that the g factor spread is the main source of the spin dephasing. Linear fits to the measured dependencies give the following values of the g factor spreads: $\Delta g_e = 0.02$ for the fast oscillations and $\Delta g_h = 0.05$ for the slow oscillations. The nonzero offset of the linear dependencies is related to other spin dephasing mechanisms as well as to the exciton recombination.

The value $|g_e| = 1.86$ for the fast oscillations is larger than the moduli of the electron g factors so far measured for QDs with emission at higher energies [3–5, 12, 13, 19–23, 25, 26]. We attribute the fast oscillations to electron spin precession. However, $|g_e| = 1.86$ is smaller than the value of $|g_e| \approx 5$ that one would expect for $E_g = 0.79$ eV from the Roth-Lax-Zwerdling relation for bulk semiconductors [34],

$$g_e(E_g) = g_0 - \frac{2E_p\Delta_{SO}}{3E_g(E_g+\Delta_{SO})}, \qquad (1)$$

where E_g is the band-gap energy, Δ_{SO} is the spin-orbit splitting of the valence band, and $E_p = 2P_{cv}^2/m_0$ is the Kane energy (P_{cv} is the interband momentum matrix element and m_0 is the free electron mass).

The origin of the slow oscillations is less evident. It may be attributed to the hole spin precession. However, the measured value of $|g_h| = 0.64$ is much larger than the transverse hole g factor measured for annealed (In,Ga)As/GaAs QDs emitting around 1.4 eV ($|g_{h\perp}| \sim 0.2$) [22]. An other possible origin of the slow oscillations might be electron spin precession in the InP substrate or in the $In_{0.53}Al_{0.24}Ga_{0.23}As$ barriers which may be initiated through two-photon absorption. A similar situation was described in Ref. [36], where electron spin precession in the GaAs buffer is superimposed on the signal from GaAs/(Al,Ga)As quantum wells.

To clarify the origin of the slow oscillations, we measured the pump power dependence of the oscillation amplitudes at $B = 1$ T. The pump power P defines the pump pulse area $\propto \int E(t)dt \propto \sqrt{P}$, where $E(t)$ is the electric field amplitude [42]. Figure 3(a) shows the dependence of the oscillation amplitude on $\sqrt{P}$ for the fast and slow oscillations. Both amplitudes have a pronounced maximum, presumably corresponding to the pulse area of π. The presence of a maximum in the dependencies indicates that the corresponding oscillations are related to the Rabi oscillations in the QD excitation, while in bulk such oscillations are hard to observe due to the fast excitation induced dephasing for elevated excitation power. Furthermore, the similar behavior for both dependencies suggests a common source for both precession frequencies. These facts exclude a barrier/substrate origin of the slow oscillations.

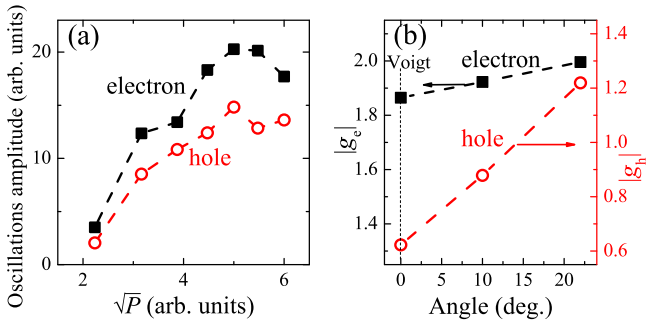

FIG. 3. (a) Dependence of the oscillation amplitudes on the square root of the pump power for the fast (solid squares) and slow (open circles) oscillations in the observed spin precessions. Broadband ~ 30 meV pump and probe beams without a pulse shaper are used. (b) Dependence of the g factor moduli on the angle between the sample surface and the magnetic field for the fast (solid squares, left axis) and slow (open circles, right axis) oscillations. The zero angle corresponds to the Voigt geometry. (a),(b) The dashed lines are guides to the eye. $B = 1$ T, the laser photon energy is 0.79 eV, and $T = 7$ K.

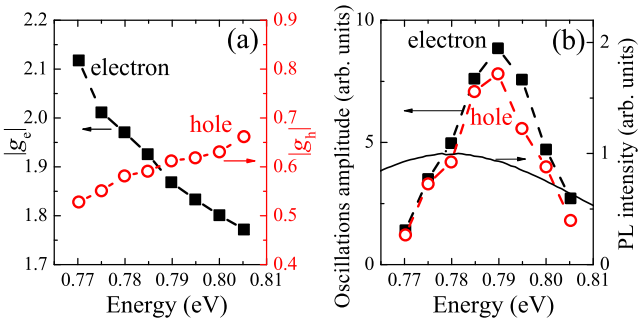

FIG. 4. Dependence of g factor moduli (a) and oscillation amplitudes (b) on the laser energy for the electron (solid squares) and hole (open circles) spin precession signal. The solid line shows the PL spectrum (right axis). (a),(b) The dashed lines are guides to the eye. $B = 1$ T, $T = 7$ K.

To further confirm the hole nature of the slow oscillations, we measured the spin dynamics for nonzero angles of the magnetic field relative to the sample surface at $B = 1$ T. It is well known that the hole g factor is strongly anisotropic in (In,Ga)As QDs [22] and can be several times higher for the magnetic field parallel to the sample growth axis than in transverse magnetic field. On the other hand, the electron g factor is more isotropic, which allows one to distinguish electron and hole spin beats. Indeed, tilting the sample with respect to the magnetic field by an angle of $\sim 20^o$ leads to a slight increase of $|g_\mathrm{e}|$ by ~ 0.1 (Fig. 3(b), left axis) compared to a significant increase of $|g_\mathrm{h}|$ by ~ 0.6 (Fig. 3(b), right axis). The large hole g factor in the studied unannealed QDs can be explained by admixing the light-hole states to the heavy-hole states as a result of strong spatial confinement.

It is interesting to examine how the electron and hole g factors are affected by the spread of QD parameters within an ensemble. The spread of QD parameters manifests itself in the inhomogeneous broadening of the PL spectrum (Fig. 1(b)). We studied the spin precessions at $B = 1$ T as functions of the laser photon energy (the laser spectral width is ~ 5 meV) which selects certain QD subsets in the whole ensemble. The energy dependence of the electron and hole g factor moduli are shown in Fig. 4(a) by the solid squares (left axis) and open circles (right axis), respectively. Interestingly, the modulus of the electron g factor decreases with energy, as reported for the electron g factor in (In,Ga)As/GaAs QDs [3, 23, 26] and GaAs/(Al,Ga)As QWs [36] and expected from Eq. (1) for negative g factors. The negative sign of the electron g factor was also proven previously for (In,Ga)As/GaAs QDs emitting at larger energies by measuring the dynamic nuclear polarization [20]. On the other hand, the modulus of the hole g factor increases with energy. Such a behavior has been reported only for holes [25].

The emission energy dependencies of the amplitudes of the electron and hole oscillations (Fig. 4(b)) show a similar peaked behavior with the maximum close to the PL maximum energy (solid line in Fig. 4(b), corresponding to the right axis), which further confirms the QD origin of both oscillations. However, the width of the dependencies (~ 20 meV) is several times smaller than the width of the PL spectrum (~ 60 meV). The comparable amplitudes of the electron and hole spin precessions indicate almost equal electron and hole populations. This fact, together with the observed oscillation decay times not exceeding the carrier population decay time (≈ 0.83 ns), suggest that the concentration of charged QDs is low and empty QDs dominate the signal despite the Si δ-doping layer.

Figure 5 summarizes the electron g factors obtained in the present work, together with the data reported in literature for III-V QDs [3, 5, 12, 13, 26, 46], as a function of the QD emission energy. The solid symbols correspond to the transverse g factors (**B** is perpendicular to the growth axis), while open symbols correspond to the longitudinal g factors (**B** is parallel to the growth axis). The solid line shows the g factor energy dependence $g_\mathrm{e}^\mathrm{bulk}(E)$ calculated for bulk semiconductors according to Eq. (1) [34]. From Fig. 5 it is clear that $g_\mathrm{e}^\mathrm{QD}(E) > g_\mathrm{e}^\mathrm{bulk}(E)$ without any exception. The deviation between QD and bulk g factors is maximal for the lowest emission energies. This deviation is presumably related to the effect of confinement on the spin-orbit coupling.

To account for the confinement effect, we calculated the energy dependence of the electron g factor using the theory of Ref. [28], which is based on the Kane's model. We use two different approaches for the QD shape: (i) a spherical QD and (ii) a flattened QD approximated by a QW. The second approach is more realistic for the studied QDs with a dome shape. The

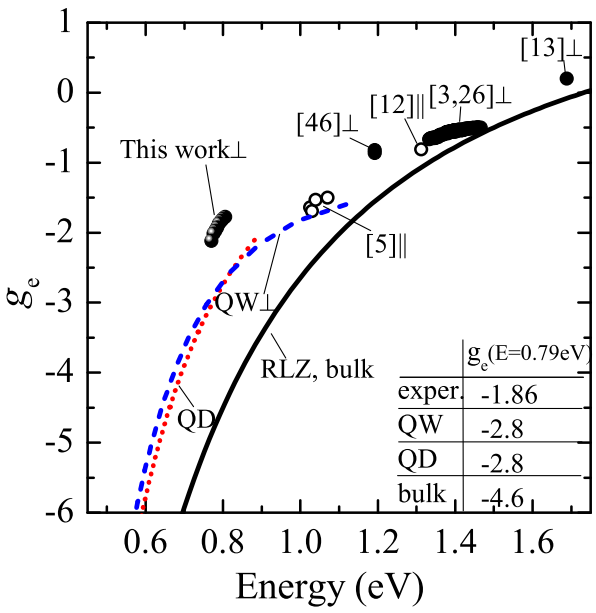

FIG. 5. Dependence of the electron g factor on the QD emission energy. The solid and open symbols correspond to the transverse and longitudinal g factors, respectively. The original data from the present work are shown together with the data from Refs. [3, 5, 12, 13, 26, 46]. The solid line shows the dependence for bulk semiconductors calculated according to the Roth-Lax-Zwerdling relation (1). The dotted and dashed lines show the dependencies calculated for spherical QDs and QWs using the model of Ref. [28]. The table shows the g factor values determined experimentally and calculated using different approaches at $E = 0.79$ eV.

QD material is assumed to be InAs with the band-gap energy $E_g = 0.417$ eV, the spin-orbit splitting of the valence band $\Delta_{SO} = 0.39$ eV, the interband matrix element $E_p = 21.5$ eV, and the heavy-hole mass $m_{hh} = 0.45m_0$ [43, 44]. A conduction- to valence-band offset ratio of $\Delta E_c/\Delta E_v = 0.6/0.4$ is used. For the $In_{0.53}Al_{0.24}Ga_{0.23}As$ barriers we used intermediate parameters between those of InAs and GaAs which are determined for the band-gap energy $E_g = 1.2$ eV by linear interpolation between the InAs and GaAs parameters as a function of the band-gap energy: $\Delta_{SO} = 0.36$ eV, $E_p = 26.7$ eV, $m_{hh} = 0.45m_0$. Linear interpolation between the InAs and GaAs parameters was also used to determine Δ_{SO} and E_p as a function of energy for calculating $g_e^{bulk}(E)$ according to Eq. (1) (the solid line in Fig. 5). In all cases we added $g_{remote} = -0.13$ to the calculated g factors to account for the contribution from the remote bands [28, 36] not included directly in the calculation. Note that for the bulk case and for spherical QDs, the longitudinal components of the g factors coincide with the transverse components.

The results of the calculations in the QD approach are shown in Fig. 5 by the dotted line and the calculated dependence for the QW approach is shown by the dashed line. Different energies for the calculated dependencies correspond to different QD radii in the QD approach and different QW widths in the QW approach. The dependencies are much closer to the experimental values than that according to Eq. (1), but a significant deviation still remains. The results are summarized in the table shown in the inset of Fig. 5. It is worth noting that the slope of the measured dependence around 0.8 eV is close to the slopes of the dependencies calculated for bulk and within the QD approach.

More realistic calculations of QD electron g factors should take into account the strain effects which might be significant for QDs emitting at energies below 1.2 eV [45]. These effects can lead to renormalization of the QD band gap and induce significant mixing of light-hole and heavy-hole states, which in turn will change the electron g factor.

IV. CONCLUSION

Using pump-probe spectroscopy we studied the spin dynamics in $InAs/In_{0.53}Al_{0.24}Ga_{0.23}As$ self-assembled quantum dots emitting in the telecom spectral range around 1.6 μm. Oscillations at frequencies corresponding to the transverse g factors $|g_e| \approx 1.9$ and $|g_h| \approx 0.6$ were observed in the ellipticity signal in a magnetic field and identified as electron and hole spin beats, respectively. The electron g factor values measured in the present work and reported previously for III-V QDs are higher than the g factors calculated for bulk semiconductors using the Roth-Lax-Zwerdling relation [34] at the same energy (note the negative sign of the g factors). The discrepancy from the Roth-Lax-Zwerdling relation increases with decreasing QD emission energy. Calculations within the Kane's model taking into account the confinement effect [28], partly reduce the discrepancy, however, an even more refined theoretical description of the experimental findings is still needed.

ACKNOWLEDGMENTS

We are grateful to E. L. Ivchenko and A. A. Kiselev for valuable advice and useful discussions and to F. Heisterkamp and A. Steinmann for technical support. We acknowledge the financial support by the Deutsche Forschungsgemeinschaft and the Russian Foundation of Basic Research in the frame of the ICRC TRR 160 as well as by the BMBF in the frame of the project Q.com-H (Contracts No. 16KIS0112 and No. 16KIS0104K). M. Bayer acknowledges support by the Government of Russia (Project No. 14.Z50.31.0021).

[1] *Spin Physics in Semiconductors*, edited by M. I. Dyakonov, (Springer-Verlag, Berlin, 2008).

[2] A. V. Khaetskii and Y. V. Nazarov, Phys. Rev. B **61**, 12639 (2000).

[3] A. Greilich, D. R. Yakovlev, A. Shabaev, Al. L. Efros, I. A. Yugova, R. Oulton, V. Stavarache, D. Reuter, A. Wieck, and M. Bayer, Science **313**, 341 (2006).

[4] G. Medeiros-Ribeiro, M. V. B. Pinheiro, V. L. Pimentel, and E. Marega, Appl. Phys. Lett. **80**, 4229 (2002).

[5] G. Medeiros-Ribeiro, E. Ribeiro, and H. Westfahl, Appl. Phys. A **77**, 725 (2003).

[6] R. M. Potok, J. A. Folk, C. M. Marcus, V. Umansky, M. Hanson, and A. C. Gossard, Phys. Rev. Lett. **91**, 016802 (2003).

[7] M. T. Björk, A. Fuhrer, A. E. Hansen, M. W. Larsson, L. E. Fröberg, and L. Samuelson, Phys. Rev. B **72**, 201307(R) (2005).

[8] M. D. Schroer, K. D. Petersson, M. Jung, and J. R. Petta, Phys. Rev. Lett. **107**, 176811 (2011).

[9] T. P. M. Alegre, F. G. G. Hernández, A. L. C. Pereira, and G. Medeiros-Ribeiro, Phys. Rev. Lett. **97**, 236402 (2006).

[10] S. Takahashi, R. S. Deacon, A. Oiwa, K. Shibata, K. Hirakawa, and S. Tarucha, Phys. Rev. B **87**, 161302(R) (2013).

[11] J. H. Prechtel, F. Maier, J. Houel, A. V. Kuhlmann, A. Ludwig, A. D. Wieck, D. Loss, and R. J. Warburton, Phys. Rev. B **91**, 165304 (2015).

[12] M. Bayer, A. Kuther, A. Forchel, A. Gorbunov, V. B. Timofeev, F. Schäfer, J. P. Reithmaier, T. L. Reinecke, and S. N. Walck, Phys. Rev. Lett. **82**, 1748 (1999).

[13] J. G. Tischler, A. S. Bracker, D. Gammon, and D. Park, Phys. Rev. B **66**, 081310(R) (2002).

[14] A. R. Goñi, H. Born, R. Heitz, A. Hoffmann, C. Thomsen, F. Heinrichsdorff, and D. Bimberg, Jpn. J. Appl. Phys. **39**, 3907 (2000).

[15] T. Nakaoka, T. Saito, J. Tatebayashi, and Y. Arakawa, Phys. Rev. B **70**, 235337 (2004).

[16] T. Nakaoka, T. Saito, J. Tatebayashi, S. Hirose, T. Usuki, N. Yokoyama, and Y. Arakawa, Phys. Rev. B **71**, 205301 (2005).

[17] N. I. Cade, H. Gotoh, H. Kamada, H. Nakano, and H. Okamoto, Phys. Rev. B **73**, 115322 (2006).

[18] N. A. J. M. Kleemans, J. van Bree, M. Bozkurt, P. J. van Veldhoven, P. A. Nouwens, R. Nötzel, A. Y. Silov, P. M. Koenraad, and M. E. Flatté, Phys. Rev. B **79**, 045311 (2009).

[19] A. Greilich, R. Oulton, E. A. Zhukov, I. A. Yugova, D. R. Yakovlev, M. Bayer, A. Shabaev, Al. L. Efros, I. A. Merkulov, V. Stavarache, D. Reuter, and A. Wieck, Phys. Rev. Lett. **96**, 227401 (2006).

[20] I. A. Yugova, A. Greilich, E. A. Zhukov, D. R. Yakovlev, M. Bayer, D. Reuter, and A. D. Wieck, Phys. Rev. B **75**, 195325 (2007).

[21] M. V. G. Dutt, J. Cheng, B. Li, X. Xu, X. Li, P. R. Berman, D. G. Steel, A. S. Bracker, D. Gammon, S. E. Economou, R. B. Liu, and L. J. Sham, Phys. Rev. Lett. **94**, 227403 (2005).

[22] A. Schwan, B. M. Meiners, A. Greilich, D. R. Yakovlev, M. Bayer, A. D. B. Maia, A. A. Quivy, and A. B. Henriques, Appl. Phys. Lett. **99**, 221914 (2011).

[23] A. Schwan, B.-M. Meiners, A. B. Henriques, A. D. B. Maia, A. A. Quivy, S. Spatzek, S. Varwig, D. R. Yakovlev, and M. Bayer, Appl. Phys. Lett. **98**, 233102 (2011).

[24] M. Syperek, D. R. Yakovlev, I. A. Yugova, J. Misiewicz, M. Jetter, M. Schulz, P. Michler, and M. Bayer, Phys. Rev. B **86**, 125320 (2012).

[25] S. A. Crooker, J. Brandt, C. Sandfort, A. Greilich, D. R. Yakovlev, D. Reuter, A. D. Wieck, and M. Bayer, Phys. Rev. Lett. **104**, 036601 (2010).

[26] J. Debus, V. F. Sapega, D. Dunker, D. R. Yakovlev, D. Reuter, A. D. Wieck, and M. Bayer, Phys. Rev. B **90**, 235404 (2014).

[27] A. Greilich, A. Shabaev, D. R. Yakovlev, Al. L. Efros, I. A. Yugova, D. Reuter, A. D. Wieck, and M. Bayer, Science **317**, 1896 (2007).

[28] A. A. Kiselev, E. L. Ivchenko, and U. Rössler, Phys. Rev. B **58**, 16353 (1998).

[29] A. V. Rodina, Al. L. Efros, and A. Y. Alekseev, Phys. Rev. B **67**, 155312 (2003).

[30] W. Sheng and A. Babinski, Phys. Rev. B **75**, 033316 (2007).

[31] J. van Bree, A. Y. Silov, P. M. Koenraad, M. E. Flatté, and C. E. Pryor, Phys. Rev. B **85**, 165323 (2012).

[32] S. Varwig, I. A. Yugova, A. René, T. Kazimierczuk, A. Greilich, D. R. Yakovlev, D. Reuter, A. D. Wieck, and M. Bayer, Phys. Rev. B **90**, 121301(R) (2014).

[33] S. Varwig, E. Evers, A. Greilich, D. R. Yakovlev, D. Reuter, A. D. Wieck, and M. Bayer, Phys. Rev. B **90**, 121306(R) (2014).

[34] L. M. Roth, B. Lax, and S. Zwerdling, Phys. Rev. **114**, 90 (1959).

[35] H. Kosaka, A. A. Kiselev, F. A. Baron, K. W. Kim, and E. Yablonovitch, Electron. Lett. **37**, 464 (2001).

[36] I. A. Yugova, A. Greilich, D. R. Yakovlev, A. A. Kiselev, M. Bayer, V. V. Petrov, Y. K. Dolgikh, D. Reuter, and A. D. Wieck, Phys. Rev. B **75**, 245302 (2007).

[37] M. Benyoucef, M. Yacob, J. P. Reithmaier, J. Kettler, and P. Michler, Appl. Phys. Lett. **103**, 162101 (2013).

[38] J. Krauth, A. Steinmann, R. Hegenbarth, M. Conforti, and H. Giessen, Opt. Express **21**, 11516 (2013).

[39] S. Varwig, A. Schwan, D. Barmscheid, C. Müller, A. Greilich, I. A. Yugova, D. R. Yakovlev, D. Reuter, A. D. Wieck, and M. Bayer, Phys. Rev. B **86**, 075321 (2012).

[40] We also checked that the form of the oscillation decay $\exp(-t/T_2^*)$, corresponding to a Lorentzian distribution of g factors, gives a comparable quality of the fit and similar fitting parameters, in particular, dephasing times, which are determined by the spread of the g factor.

[41] I. A. Merkulov, Al. L. Efros, and M. Rosen, Phys. Rev. B **65**, 205309 (2002).

[42] M. S. Scully and M. O. Zubairy, *Quantum Optics* (Cambridge University Press, U.K., 1997).

[43] I. Vurgaftman, J. R. Meyer, and L. R. Ram-Mohan, J. Appl. Phys. **89**, 5815 (2001).

[44] S. Adachi, *Physical Properties of III-V Semiconductor Compounds* (Wiley, New York, 1992).

[45] A. Kiselev, K. Kim, and E. Ivchenko, Phys. Status Solidi B **215**, 235 (1999).

[46] We also studied the spin precession in a transverse magnetic field for InAs/GaAs self-assembled QDs grown by molecular-beam epitaxy on a (001)-oriented GaAs substrate and emitting at a wavelength of about 1 μm. Two samples were considered, one annealed at $T_{\rm ann} = 800$ ^{o}C and the other one at 820 ^{o}C for half a minute. Both samples are pumped and probed by Yb:KGW 400 fs laser pulses at an energy of 1.192 eV. The sample annealed at 800 ^{o}C reveals electron spin precession with $|g_{\rm e}| = 0.86$, while for the sample annealed at 820 ^{o}C, the electron g factor $|g_{\rm e}| = 0.82$.